

Intramolecular Excimer Formation of *meso*- and *rac*-2,4-Di(2-pyrenyl)pentane and *meso*- and *rac*-Bis[1-(2-pyrenyl)ethyl] Ether

P. Collart, S. Toppet, and F. C. De Schryver*

Chemistry Department, KULeuven, Celestijnlaan 200 F, B-3030 Heverlee-Leuven, Belgium. Received July 7, 1986

ABSTRACT: The excited-state kinetics of the diastereoisomers of 2,4-di(2-pyrenyl)pentane and bis[1-(2-pyrenyl)ethyl] ether are investigated in isooctane. A conformational analysis performed by ^1H NMR reveals the conformational distribution within each configuration of 1,4-di(2-pyrenyl)pentane. With the use of stationary and nonstationary fluorescence techniques, kinetic and thermodynamic parameters of intramolecular excimer formation are obtained for each of the diastereoisomers of both compounds.

Introduction

During the past few years, research on the photophysics of 2,4-diarylpentanes¹⁻³ and bis(1-arylethyl) ethers^{4,5} has led to a better understanding of the photophysics of polychromophoric systems such as vinyl polymers.⁶ The possibility of forming an intramolecular excimer is governed by two different requirements:⁷ first, the rate constant of excimer formation has to be competitive with the radiative and nonradiative decay of the locally excited state; and second, the change in free enthalpy has to be favorable. For a given chromophore, the position of substitution seems to have an important effect on the excited-state kinetics. This is shown by comparing the results of the study of 2,4-di(1-pyrenyl)pentane (D1PP) and bis[1-(1-pyrenyl)ethyl] ether (B1PEE)⁸ with those in this work and in work done by Zachariasse.⁹ The study of 2,4-disubstituted pentanes has an additional important advantage compared to 1,3-disubstituted propanes. The meso and racemic diastereoisomers, which can be looked at as model compounds for vinyl polymers, may permit insight into the influence of tacticity and into the excited-state molecular dynamics of these polymers. Furthermore, the excimer kinetics can be correlated with a number of low-energy conformations that can be determined by ^1H NMR. The meso diastereoisomer, at room temperature and below, is present in only one ground-state chain conformation, while the racemic diastereoisomer is present in two ground-state chain conformations.¹⁰ In this work, the photophysics of *meso*- and *rac*-2,4-di(2-pyrenyl)pentane (D2PP) and *meso*- and *rac*-bis[1-(2-pyrenyl)ethyl] ether (B2PEE) is described.

Experimental Section

The synthesis of D2PP began with 2-pyrenecarboxaldehyde (1) and 2-acetylpyrene (2)^{11,12} to form 1,3-di(2-pyrenyl)-2-propen-1-one (3). Compounds 2 (10 g) and of 1 (9.43 g) are dissolved in 500 mL of ethanol containing 2.5 g of sodium hydroxide. The reaction mixture is stirred at 40 °C for 24 h. Upon cooling, the chalcone 3 precipitates and is purified through recrystallization from a minimum amount of benzene in which it is dissolved and to which petroleum ether is added. Compound 3 was reacted with methylmagnesium iodide in the presence of an equivalent amount of cuprous chloride in ether to obtain 1,3-di(2-pyrenyl)butan-1-one (4). Ketone 4 was again reacted with methylmagnesium iodide to form 2,4-di(2-pyrenyl)-2-pentanol (5). To a solution of 28.2 g of methylmagnesium iodide in ether is added in small portions 8 g of solid 4. The mixture is heated at reflux for 2 h, cooled, and hydrolyzed with a concentrated ammonium chloride solution. The organic solvent layer is separated, washed with a dilute sodium carbonate solution, dried, and evaporated. The crude reaction product 5 is purified by column chromatography on silica gel with benzene as eluent. Compound 5 was reduced with hydrogen on a Pd/C catalyst in acetic acid

to obtain D2PP. To a solution of 0.5 mL of concentrated hydrochloric acid in 50 mL of acetic acid 1 g of 5 and 0.02 g Pd/C (10%) is added. The reaction mixture is shaken in a Parr hydrogenation apparatus for 48 h under 2.5 atm of hydrogen. The catalyst is removed by filtration and the crude reaction product is extracted with ether. The ether layer is washed with sodium carbonate and dried and the ether evaporated. The crude product is purified, and the diastereoisomers are separated by column chromatography on silica gel with a hexane(97)-tetrahydrofuran(3) mixture as eluent. A further purification was performed by HPLC on silica with the same eluent mixture.

The synthesis of B2PEE to give *meso*- and *rac*-D2PP (m/e 472 (M^{+})), 243, 229, 201) began with 2-pyrenecarboxaldehyde, which was converted into 1-(2-pyrenyl)ethanol using a solution of methylmagnesium iodide in ether. The 1-(2-pyrenyl)ethanol was then used to obtain *meso*- and *rac*-B2PEE (m/e 474 (M^{+})), 230, 215, 201) according to a method described in the literature.⁵ The separation and purification of the diastereoisomers was done with HPLC (Doucel-Chiralpac (+)OT and 95% hexane/5% 2-propanol were used for *meso*- and *rac*-D2PP; J. T. Baker silica gel 5 μm and 80% toluene/20% hexane were used in the case of *meso*- and *rac*-B2PEE). The ^1H NMR measurements were performed on a Bruker 250-MHz NMR spectrometer. Absorption measurements were performed on a Perkin-Elmer UV/vis Lambda 5 spectrophotometer. The fluorescence spectra were recorded on a SPEX Fluorolog and were corrected for the wavelength dependence of the photomultiplier. The time-correlated single-photon-counting technique (tcspc) was used to perform the transient measurements. Details of the experimental setup are described elsewhere.^{13,14} All absorption and fluorescence measurements were done in isooctane (Merck UVASOL).

Results and Discussion

The absorption spectra of *meso*- and *rac*-D2PP are identical with those of 2-isopropylpyrene, which was used as a reference compound. Similarly, the absorption spectra of *meso*- and *rac*-B2PEE are identical with those of 1-(2-pyrenyl)ethyl ethyl ether, which was used as a reference compound (Figure 1). Ground-state interactions between the two chromophores of *meso*- and *rac*-D2PP and of *meso*- and *rac*-B2PEE are therefore negligible. Furthermore, no excitation wavelength effect is observed in the emission spectra of the diastereoisomers of both compounds. The ground-state conformational distribution of D2PP was studied by ^1H NMR according to the method described by Bovey.¹⁵ The conformational distribution of B2PEE is discussed by comparing the ^1H NMR data with those of D2PP. The ^1H NMR data are given in Table I. The meso diastereoisomer of D2PP is always found to be about 100% in the TG conformation (Figure 1). The racemic diastereoisomer is present in two ground-state conformations: TT and GG (Figure 2). In both deuterated cyclohexane and deuterated chloroform, at room temperature, the TT conformation of racemic D2PP is

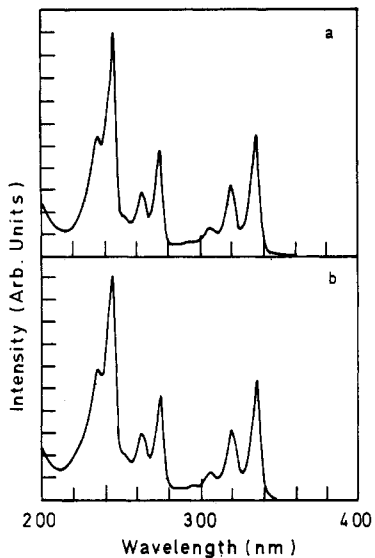


Figure 1. Absorption spectra of 2-isopropylpyrene (a) and 1-(2-pyrenyl)ethyl ethyl ether (b) at room temperature in isoctane.

Table I
¹H NMR Data of *meso*- and *rac*-D2PP and B2PEE in Deuterated Chloroform at Room Temperature (Me₃Si as Reference)

δ , ppm	multiplicity	origin	J , Hz
<i>meso</i> -D2PP			
1.56	d	CH ₃	$^3J = 6.7$
2.28	ABX ₂	CH ₂	$^3J_{BX} = 7.5$
2.48	ABX ₂		$^3J_{AX} = 7.0$
3.18	ABX ₂	CH	$^2J_{AB} = -13.5$
7.96–8.15	m	aryl -H	$^2J_{AB} = -13.5$
<i>rac</i> -D2PP			
1.45	d	CH ₃	$^3J = 6.7$
2.31	AA'XX'	CH ₂	$^3J_{AX} = 10.0$
2.95	AA'XX'	CH	$^3J_{AX} = 5.3$ $^2J_{AA} = 13.4$ $^4J_{XX} \approx 0$
7.95–8.20	m	aryl H	
<i>meso</i> -B2PEE			
1.77	d	CH ₃	$^3J = 6.1$
5.07	q	CH	$^3J = 6.1$
7.88–8.10	m	aryl H	
<i>rac</i> -B2PEE			
1.65	d	CH ₃	$^3J = 6.3$
4.77	q	CH	$^3J = 6.3$
7.99–8.1	m	aryl H	

predominant: 80% TT and 73% TT, respectively. The observed solvent effect on the conformational distribution is similar but smaller than that found for D1PP.⁸ These results agree quite well with those obtained on similar compounds.^{3,8,15,16} A comparison of the ¹H NMR data for the aromatic protons of *meso*-B2PEE with those of *meso*-D2PP reveals no major differences, indicating that the conformational distribution of *meso*-B2PEE is not significantly different from that of *meso*-D2PP (Figure 2). In the NMR data for the racemic diastereoisomers one important difference appears. The position of the singlet absorption signal of H₁ is shifted significantly to more shielded δ values for *rac*-B2PEE compared with *rac*-D2PP. The position of the H₁ protons in the ¹H NMR spectrum is a function of the contribution of the TT conformation, since these protons are shielded by the mutual ring-current effect of the pyrene chromophores in the TT conformation. It can therefore be concluded that the equilibrium between TT and GG in the case of *rac*-B2PEE is shifted more toward the GG conformation compared to *rac*-D2PP. This

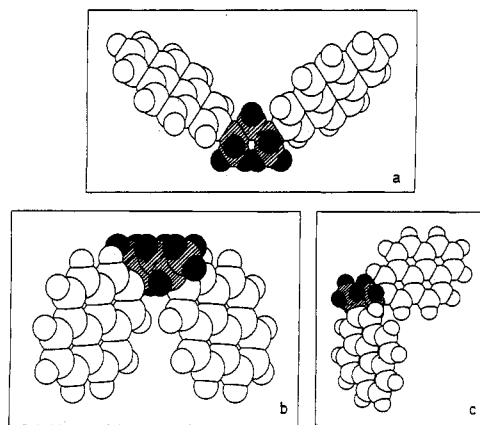


Figure 2. Low-energy ground-state conformations of *rac*-D2PP (a) GG; (b) TT and *meso*-D2PP (c) TG.

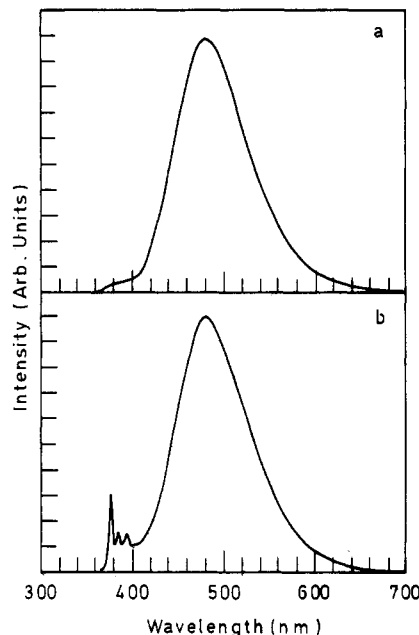


Figure 3. Corrected Fluorescence spectra of *meso*- (a) and *rac*-D2PP (b) at room temperature in isoctane.

can be explained by comparing the bond lengths of the C–O bond in B2PEE and the C–C bond in D2PP. The shorter ether bond induces a stronger 1,4-interaction between the methine hydrogens and the pyrene chromophores in B2PEE. This causes a shift of the conformational equilibrium from TT to GG.

The fluorescence properties and the excited-state kinetics will be discussed separately for both diastereoisomers.

***meso*-D2PP and *meso*-B2PEE.** The steady-state fluorescence spectra of *meso*-D2PP and *meso*-B2PEE at room temperature show mainly excimer fluorescence with an emission maximum at 485 nm (Figures 3 and 4). This maximum shifts from 480 nm at 343 K to 495 nm at 203 K. The frequency width at half-height varies from 4100 to 3600 cm⁻¹ over the same temperature interval. This can be explained in terms of the population of higher vibrational levels of the excimer state. The frequency width at half-height of *meso*-D1PP however is considerably larger,⁸ suggesting the presence of only one excimer in the case *meso*-D2PP. A similar effect is observed on comparing the spectra of B1PEE and *meso*-B2PEE. Progressively lowering the temperature (from 298 to 203 K) leads to an increase in monomer fluorescence and a decrease in excimer fluorescence.

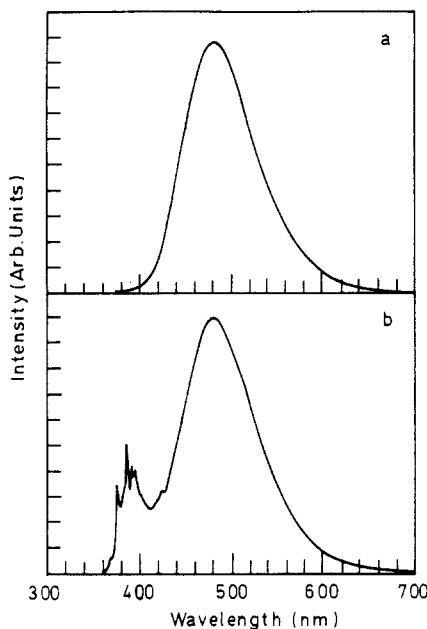


Figure 4. Corrected fluorescence spectra of *meso*- (a) and *rac*-B2PEE (b) at room temperature in isoctane.

Table II
Decay Parameters of *meso*- and *rac*-D2PP and B2PEE at Room Temperature in Isoctane

aw, ^a nm	α_1	λ_1^{-1}	α_2	λ_2^{-1}	χ^2_r	DW ^b
500	-0.49	1.0	0.51	141.4	1.13	1.89
378 ^c						
500	-1.44	11.8	1.52	136	1.07	1.95
378	1.12	11.9	0.02	134	1.19	1.80
500	0.86	0.3	0.81	88	1.08	1.80
378 ^c						
500	-1.29	20.8	1.32	83	1.18	2.35
378	0.26	21.3	0.06	87	1.14	1.91

^a Analysis wavelength. ^b The meaning of the reduced χ^2 and Durbin-Watson statistical tests is explained in ref 12. ^c Due to the low fluorescence intensity at this wavelength, the decay parameters could not be determined accurately.

The time dependence of the fluorescence was studied by the time-correlated single-photon-counting method. The fluorescence decays were monitored at 377 nm for the monomer fluorescence and at 500 nm for the excimer fluorescence. In the temperature region between 253 and 343 K only the excimer fluorescence decay could be adequately measured owing to the low fluorescence intensity of the locally excited state. The excimer fluorescence decay of *meso*-D2PP and *meso*-B2PEE can be analyzed as a difference of two exponentials throughout the excimer band (Table II). This also indicates the presence of only one excimer species in both compounds. This contrasts with the fluorescence decays in the excimer region of *meso*-D1PP and *meso*-B1PEE, which could only be analyzed as a triple-exponential function.⁸ This analysis proved the presence of two excimer species with different spectral distributions in the case of *meso*-D1PP and *meso*-B1PEE.⁸ At low temperature (203 to 183 K) the monomer fluorescence decay of *meso*-B2PEE can be fitted to a single-exponential decay law (Figure 5). The decay parameter obtained in the analysis of the monomer fluorescence corresponds to one of the parameters in the excimer decay. Up to now, however, we have not been able to analyze the monomer fluorescence of *meso*-D2PP as a single exponential at temperatures below 203 K. Repeated measurements indicate this is due to an impurity. One cannot, however, exclude the possibility that the additional

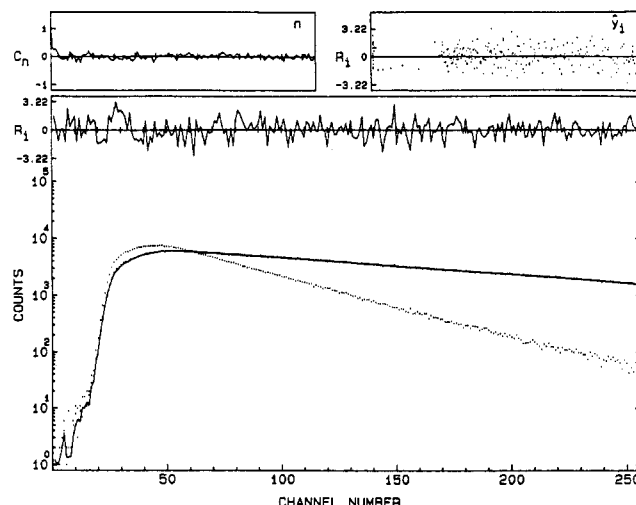


Figure 5. Fluorescence decay curve of *meso*-B2PEE at 203 K in isoctane ($\lambda_{\text{exc}} = 330$ nm, $\lambda_{\text{anal}} = 377$ nm, channel width = 0.074 ns, $\lambda_1^{-1} = 5.6$ ns, $\chi^2_r = 1.18$, Durbin-Watson = 1.76).

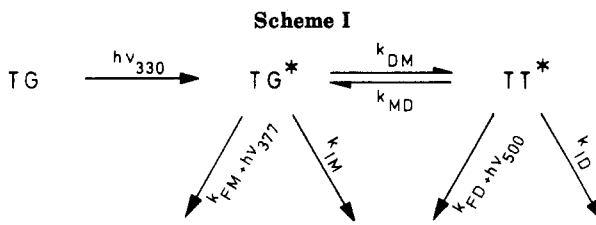


Table III
Kinetic and Thermodynamic Parameters of *meso*- and *rac*-D2PP and B2PEE in Isoctane

parameter	meso compound	
	D2PP	B2PEE
E_{DM} , kJ mol ⁻¹	16 ± 2	18 ± 2
k^o_{DM} , s ⁻¹	$(8.4 \pm 0.9) \times 10^{11}$	$(5.4 \pm 0.5) \times 10^{12}$
E_{MD} , kJ mol ⁻¹	32 ± 6	39 ± 8
k^o_{MD} , s ⁻¹	$(1.2 \pm 0.3) \times 10^{14}$	$(1.4 \pm 0.3) \times 10^{15}$
ΔH_0 , kJ mol ⁻¹	116 ± 8	-21 ± 10
ΔS_0 , J mol ⁻¹ K ⁻¹	-42 ± 18	-46 ± 14
parameter	racemic compound	
	D2PP	B2PEE
E_{obsd} , ^b kJ mol ⁻¹	20 ± 2	22 ± 2
k^o_{obsd} , ^a s ⁻¹	$(1.8 \pm 0.2) \times 10^{11}$	$(3.3 \pm 0.3) \times 10^{11}$
E_{MD} , kJ mol ⁻¹	34 ± 5	40 ± 8
k^o_{MD} , s ⁻¹ (a)	$(5.0 \pm 1) \times 10^{13}$	$(3 \pm 2) \times 10^{14}$
ΔH_0 , kJ mol ⁻¹	-14 ± 7	-18 ± 10
ΔS_0 , J mol ⁻¹ K ⁻¹	-47 ± 12	-57 ± 30

^a Preexponential factor in the Arrhenius equation. ^b Determined in the linear portion of the Arrhenius plot at low temperature (243–203 K).

component in the decay curve of the monomer fluorescence of *meso*-D2PP is caused by the presence of a small amount of the TT conformation, which forms an excimer immediately after excitation without any significant conformational change. The sum of the preexponentials in the excimer decays equals zero within experimental error. From these results it was concluded that the molecular dynamics of *meso*-D2PP and *meso*-B2PEE can be represented by Scheme I.^{1,3} In the ground state only one conformation is present (TG) that can reach the excimer conformation (TT) through one 120° rotation in the backbone chain. At low temperature, the dissociation of the excimer (k_{MD}) becomes negligible compared to the decay of the excimer leading to the single-exponential decay observed in the fluorescence analysis. The notation used in Scheme I is the same as that used for intermole-

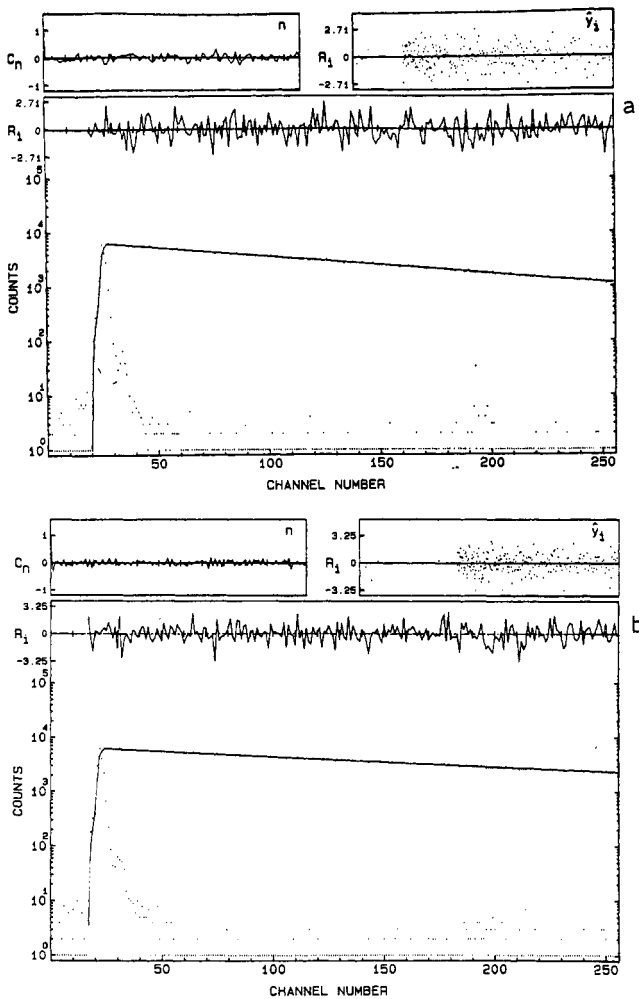
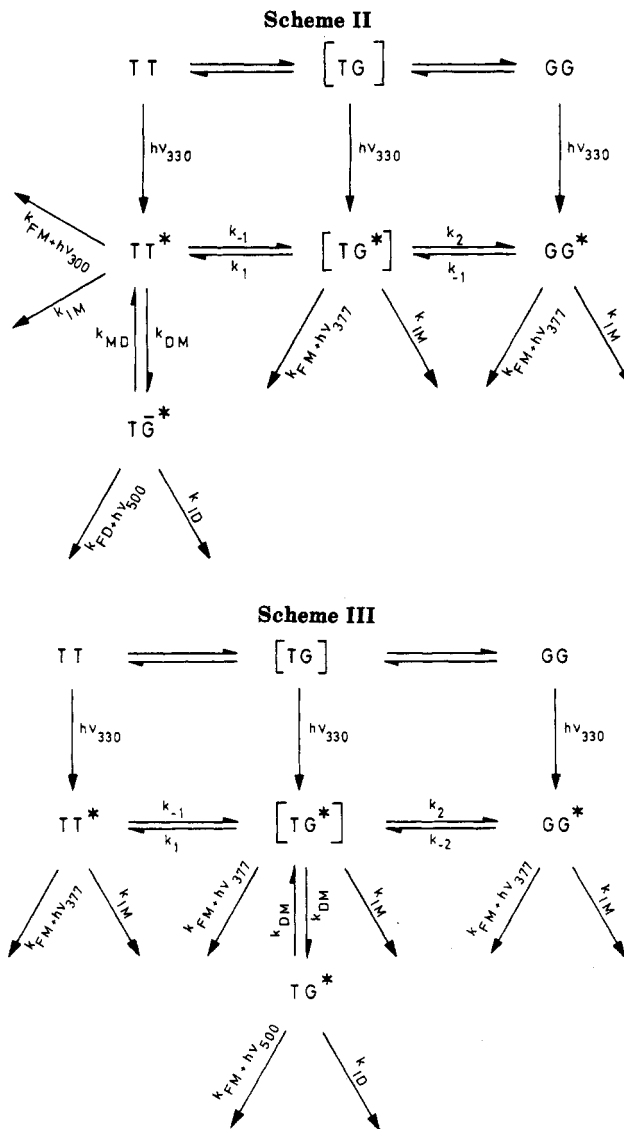


Figure 6. Fluorescence decay curves of *rac*-D2PP (a) and *rac*-B2PEE (b) in isoctane at 220 K: (a) $\lambda_{\text{exc}} = 330 \text{ nm}$, $\lambda_{\text{anal}} = 377 \text{ nm}$, channel width = 1.404 ns, $\lambda^{-1} = 187.3 \text{ ns}$, $\chi^2 = 1.04$, Durbin-Watson = 1.96; (b) $\lambda_{\text{exc}} = 330 \text{ nm}$, $\lambda_{\text{anal}} = 377 \text{ nm}$, channel width = 1.404 ns, $\lambda^{-1} = 321.0 \text{ ns}$, $\chi^2 = 1.07$, Durbin-Watson = 2.24.

cular excimer kinetics by Birks.¹⁷ A summary of the kinetic data is given in Table III.

***rac*-D2PP and *rac*-B2PEE.** The steady-state fluorescence spectra of *rac*-D2PP and *rac*-B2PEE have a feature in common with the meso diastereoisomers of D2PP and B2PEE (Figures 3 and 4). The excimer fluorescence band is completely superimposable at all temperatures investigated, suggesting an identical geometrical structure of the excimer. As the temperature decreases, the increase of monomer fluorescence and the decrease of excimer fluorescence is more pronounced compared to the meso diastereoisomer. The fluorescence decay curves monitored at 377 and 500 nm can be described by the same decay laws used for *meso*-D2PP and *meso*-B2PEE. The monomer fluorescence decays can be analyzed as a double-exponential decay function in the temperature domain between 298 and 233 K. Below this temperature the decays are single exponential (Figure 6). There is good agreement between the decay parameters in the monomer and excimer decay, and the sum of the preexponentials in the excimer decay equals zero within experimental error. Figure 6 clearly indicates that there is no short component in the fluorescence decay. It should also be pointed out that identical decay parameters were obtained when the fluorescence decay was measured over several decades. The experimental parameters of the fluorescence decays of *rac*-D2PP and -B2PEE at room



temperature are given in Table II.

The molecular dynamics of the racemic diastereoisomer upon excitation is more complicated due to the presence of two ground-state conformations. Since the decay laws used for *meso*-D2PP can also be applied to the racemic diastereoisomer, all the rate constants describing the equilibrium between the ground-state conformations must be large compared to the rate constant of excimer formation. However, the question still remains: from which conformation does excimer formation take place? It is not likely that it occurs directly from the GG conformation. This would mean a simultaneous rotation around two bonds and would be associated with a relatively high activation barrier. One possibility is that excimer formation takes place from the TT conformation. This possibility is depicted in Scheme II.

A third route could be excimer formation starting from the TG conformation (Scheme III). This intermediate conformation between the TT and GG conformation has a relatively high energy content owing to an unfavorable interaction between the methyl group and the pyrene moiety. In the study of the 1,3-di(*N*-carbazolyl)propane the effect of a ground-state preequilibrium on the kinetic data has been evaluated.³ When this preequilibrium is taken into account, the rate constants and activation barriers of excimer formation can be rewritten with the following equations:

If Scheme II is considered

$$k_{\text{obsd}} = f_{\text{TT}} k_{\text{DM}} \quad (1)$$

$$f_{\text{TT}} = \frac{K_1 K_2}{1 + K_1 + K_1 K_2} \quad (2)$$

$$K_1 = k_1/k_{-1} \quad (3)$$

$$K_2 = k_{-2}/k_2 \quad (4)$$

$$E_{\text{obsd}} = E_{\text{DM}} + \frac{\Delta H_2^\circ + (1 + K_2)\Delta H_1^\circ}{1 + K_1 + K_1 K_2} \quad (5)$$

If Scheme III is considered

$$k_{\text{obsd}} = f_{\text{TG}} k_{\text{DM}} \quad (6)$$

$$f_{\text{TG}} = \frac{K_2 K_3}{K_2 + K_3 + K_2 K_3} \quad (7)$$

$$K_3 = k_{-1}/k_1 = 1/K_1 \quad (8)$$

$$E_{\text{obsd}} = E_{\text{DM}} + \frac{\Delta H_2^\circ + \Delta H_3^\circ}{K_2 + K_3 + K_2 K_3} \quad (9)$$

In these schemes k_{obsd} and E_{obsd} are the observed rate constant and activation barrier of excimer formation, respectively. The fractions of the TT or TG conformations at a given temperature are represented by f_{TT} and f_{TG} .

The rate constants for conformational change are considered identical in the ground and excited states. Although the lack of information concerning the equilibrium in the ground state prevents a distinction between Scheme II and Scheme III, it is tentatively possible to use data obtained for similar compounds, the 2,4-diphenylpentanes, which have been thoroughly studied with regard to ground-state thermodynamics and kinetics.^{15,18,19} If these data are applied to the above equations the following results are obtained: the additional term in the expression of the observed activation energy (eq 5) according to Scheme II equals -4 kJ/mol while in Scheme II (eq 9) it equals 14.5 kJ/mol.

A further distinction can be made by considering the temperature dependence of the rate constants of excimer formation in both cases. In the case of Scheme II it can be assumed that the fraction of the TT conformation is considerable and decreases with increasing temperature. Scheme II should therefore lead to a negative deviation from linearity in the Arrhenius plot of the rate constant of excimer formation. In Scheme III, however, the fraction of the TG conformation is considered small at all temperatures since it is not a low-energy conformation. No deviation from linearity should then be observed. The observation of an important negative deviation from linearity in the Arrhenius plot led us to conclude that Scheme II is valid in the case of *rac*-D2PP and *rac*-B2PEE (Figure 7). The kinetic and thermodynamic data of D2PP and B2PEE are summarized in Table III. If the linear part of the Arrhenius plot is extrapolated to higher temperatures, an estimate of f_{TT} can be made. The assumption is that the extrapolated rate constants at all temperatures studied are equal to the value of k_{DM} . The variation of f_{TT} with temperature in the high-temperature region (303–343 K) can then be used to determine ΔH_0 and ΔS_0 for the conformational equilibrium between TT and GG of the racemic diastereoisomer. In the case of *rac*-D2PP their values are 12.2 kJ mol⁻¹ and 35 J mol⁻¹ K⁻¹, respectively. In the case of racemic B2PEE their values are 5 kJ mol⁻¹ and 12 J mol⁻¹ K⁻¹, respectively. The conformational distribution between TT and GG can then be calculated

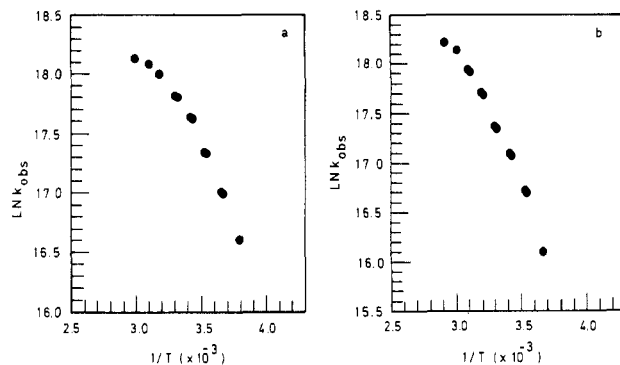


Figure 7. Arrhenius plot of the rate constant of excimer formation of *rac*-D2PP (a) and *rac*-B2PEE (b).

and equals 70% TT and 30% GG for *rac*-D2PP and 61% TT and 39% GG for *rac*-B2PEE at room temperature.

The activation barrier found for the racemic diastereoisomer is somewhat higher than that observed for the meso isomer owing to steric hindrance between the pyrene moieties during the rotation process to the excimer conformation. The difference between the values of k°_{DM} and k°_{obsd} of the meso and racemic diastereoisomers of each compound can be explained by a more organized transition state in the case of the racemic diastereoisomer. This can be well understood by comparing the meso TG and the racemic TT conformation in Figure 2. Since the pyrene groups are already parallel in the transition state of the racemic diastereoisomer, which is not the case for the meso diastereoisomer, a lower value for the preexponential factor in the Arrhenius equation (k°_{DM} and k°_{obsd}) will result. The lower value of ΔH_0 for the excimer in *rac*-D2PP is caused by the less favorable chain conformation imposed upon excimer formation. The ΔS_0 values for the racemic diastereoisomers can be expected to be higher than for the meso ones since two ground-state conformations are present upon excitation. The observation of a small difference between the ΔS_0 values is attributed to the fact that k°_{DM} for the racemic isomer is determined from the low-temperature region of the Arrhenius plot (243–203 K), where the TT conformation is assumed to predominate. The higher values of ΔH_0 , in general, for meso- and *rac*-B2PEE are explained by the shorter ether bond in B2PEE. The stabilizing interaction energy between the pyrene groups results in a larger stabilization of the excimer.

Conclusion

Knowledge of the ground-state conformational equilibrium is helpful in understanding the excited-state molecular dynamics. Comparing the results of meso- and *rac*-D2PP and B2PEE with those of meso- and *rac*-D1PP and B1PEE⁸ shows that the complexity of the excited-state kinetics is strongly related to the substitution pattern of the chromophore.²⁰ This complexity is caused by the number of possible orientations of the chromophore with regard to the chain.⁸ If the bond between the chromophore and the chain is in line with a C₂ axis of the chromophore (e.g., 2-pyrenyl) the number of orientations is limited and rotation of the chromophore around 180° produces an identical orientation. If this condition is not fulfilled (e.g., 1-pyrenyl) the number of orientations of the chromophore will be higher, resulting in a more complex excited-state behavior. The compounds studied in this work are the first for which thermodynamic parameters of both diastereoisomers could be compared.

Acknowledgment. P.C. thanks the IWONL and the KULeuven for a doctoral fellowship. We thank the FKFO

for financial support of the laboratory. Dr. N. Boens and G. Desie are thanked for their contribution in the development of the tcspc analysis program.

References and Notes

- De Schryver, F. C.; Moens, L.; Van der Auweraer, M.; Boens, N.; Monnerie, L.; Bokobza, L. *Macromolecules* 1982, 15, 64.
- Ito, S.; Yamamoto, M.; Nishijima, Y. *Bull. Chem. Soc. Jpn.* 1981, 54, 35.
- Vandendriessche, J.; Palmans, P.; Toppet, S.; Boens, N.; De Schryver, F. C.; Masuhara, H. *J. Am. Chem. Soc.* 1984, 106, 8057.
- De Schryver, F. C.; Demeyer, K.; Van der Auweraer, M.; Quanten, E. *Ann. N.Y. Acad. Sci.* 1981, 366, 93.
- Becker, H. D.; Anderson, K. *J. Org. Chem.* 1982, 47, 354.
- Semerak, S. N.; Frank, C. W. *Adv. Polym. Sci.* 1984, 54, 31.
- De Schryver, F. C.; Boens, N.; Put, J. *Adv. Photochem.* 1977, 10, 359.
- Collart, P.; Toppet, S.; Zhou, Q. F.; Boens, N.; De Schryver, F. C. *Macromolecules* 1985, 18, 1026.
- Zachariasse, K. A.; Busse, R.; Duveneck, G.; Kuhnle, W. *J. Photochem.* 1985, 28, 237.
- De Schryver, F. C.; Vandendriessche, J.; Demeyer, K.; Collart, P.; Boens, N. *Polym. Photochem.* 1985, 6, 215.
- Vollmann, H.; Becker, H.; Correll, M.; Streck, H.; *Justus Liebigs Ann. Chem.* 1937, 531, 1.
- Nakasui, K.; Akiyama, S.; Nakagawa, M. *Bull. Chem. Soc. Jpn.* 1972, 45, 875.
- Desie, G.; Boens, N.; Van den Zegel, M.; De Schryver, F. C. *Anal. Chim. Acta* 1985, 170, 45.
- Van den Zegel, M.; Boens, N.; Daems, D.; De Schryver, F. C. *Chem. Phys.* 1986, 101, 311.
- Bovey, F. A.; Hood, F. P., III; Anderson, E. W.; Snyder, L. C. *J. Chem. Phys.* 1965, 42, 3900.
- Ito, S.; Yamamoto, M.; Nishijima, Y. *Bull. Chem. Soc. Jpn.* 1982, 55, 363.
- Birks, J. B.; Dyson, D. J.; Munro, I. H. *Proc. R. Soc. London* 1963, 275, 36.
- Gorin, S.; Monnerie, L. *J. Chim. Phys. Physicochim. Biol.* 1970, 67, 869.
- Froelich, B.; Noel, C.; Jasse, B.; Monnerie, L. *Chem. Phys. Lett.* 1976, 44, 159.
- De Schryver, F. C.; Collart, P.; Vandendriessche, J.; Goedeweck, R.; Swinnen, A. M.; Van der Auweraer, M. *Acc. Chem. Res.*, in press.

Plasticization of Poly(butyral-co-vinyl alcohol)

Jacob Schaefer,^{*†} Joel R. Garbow,[‡] and E. O. Stejskal[§]

Physical Sciences Center, Monsanto Company, St. Louis, Missouri 63167

J. A. Lefelar

Monsanto Chemical Company, Springfield, Massachusetts 01151.
Received October 10, 1986

ABSTRACT: The partitioning of polymer and plasticizer into soft and hard regions for mixtures of poly(butyral-co-vinyl alcohol) and dihexyl adipate has been determined by magic-angle-spinning ¹³C NMR. The soft regions are detected by Fourier-transform techniques with scalar decoupling and the hard regions by cross-polarization with dipolar decoupling. This two-phase character of plasticized polybutyral is also observed in small-angle neutron scattering experiments in which integrated scattering intensity increases linearly with plasticizer concentration. We attribute the soft regions to liquid plasticizer containing mobile polymer and the hard regions to solid polymer associated with partially immobilized plasticizer. There is no chemical exchange between hard and soft regions on a 1-s time scale. The frequencies but not the amplitudes of cooperative main-chain motions of the polymer in the hard regions are influenced by interactions with the soft regions. This result is incorporated into a two-phase domain model that is used to rationalize the macroscopic stress-relaxation properties of these plasticized polymers.

Introduction

A plasticizer is a liquid that is soluble in a glassy polymer, lowers the glass transition of the polymer, and reduces its modulus.¹ Mechanisms of plasticization are not detailed, but the conventional model envisions a homogenous, dynamic interaction between polymer and diluent, resulting in reduced chain-chain interactions, reduced local viscosity, and increased microscopic chain mobility.² This is especially true at low diluent concentration. At higher concentrations, depending on polymer-diluent compatibility, phase separation may occur, with diluent association apparent in mechanical and dielectrical response.³ The system is now heterogeneous, with variations in the degree of plasticization of the polymer depending upon local conformation, or, for copolymers, composition.

We have examined the plasticization of poly(butyral-co-vinyl alcohol) (78 wt % polybutyral, known commer-

cially as Butvar) by dihexyl adipate using Fourier-transform (FT) ¹³C NMR, cross-polarization (CP) magic-angle-spinning (MAS) ¹³C NMR, and small-angle neutron scattering (SANS). The results are not consistent with the conventional picture of plasticization. Even at low levels of plasticizer, this system is heterogeneous, consisting of microscopic soft regions of liquid diluent containing dissolved polymer, embedded in a hard matrix of solid polymer associated with immobilized plasticizer. The partitioning between the two types of regions persists with increasing levels of plasticizer. We have found that mechanical, thermal, and chain-dynamics measurements can be described in terms of the interactions within and between these soft and hard regions.

Experiments

Magic-Angle Spinning. Carbon-13 MAS spectra and relaxation measurements were made on a spectrometer built around a 12-in. iron magnet operating at a proton Larmor frequency of 60 MHz.⁵ The magic-angle rotor (Figure 1) is of the double-bearing type,⁶ in which a cylindrical sample chamber is supported between two cylindrical gas journal bearings.⁷ The rotor is held in position by a gas thrust bearing at one end, perpendicular to the rotation axis. The rotor is driven by an array of tangential

[†]Present address: Department of Chemistry, Washington University, St. Louis, MO 63130.

[‡]Present address: Monsanto Company, Life Sciences NMR Center, Chesterfield, MO 63198.

[§]Present address: Department of Chemistry, North Carolina State University, Box 8204, Raleigh, NC 27695.